Journal of ELECTRONIC MATERIALS, Vol. 38, No. 5, 2009
DOI: 10.1007/s11664-009-0689-3

Regular Issue Paper

Creep Behavior of Lead-Free Sn-Ag-Cu + Ni-Ge Solder Alloys

N. HIDAKA,[1,3] H. WATANABE,[1] and M. YOSHIBA[2]

1.—Production Technology Laboratory, Fuji Electric Advanced Technology Co., Ltd., 1, Fuji-machi, Hino-city, Tokyo 191-8502, Japan. 2.—Department of Mechanical Engineering, Graduate School of Science and Engineering, Tokyo Metropolitan University, 1, Minami-Osawa, Hachioji, Tokyo 192-0397, Japan. 3.—e-mail: hidaka-noboru@fujielectric.co.jp

We developed a new lead-free solder alloy, an Sn-Ag-Cu base to which a small amount of Ni and Ge is added, to improve the mechanical properties of solder alloys. We examined creep deformation in bulk and through-hole (TH) form for two lead-free solder alloys, Sn-3.5Ag-0.5Cu-Ni-Ge and Sn-3.0Ag-0.5Cu, at elevated temperatures, finding that the creep rupture life of the Sn-3.5Ag-0.5Cu-Ni-Ge solder alloy was over three times better than that of the Sn-3.0Ag-0.5Cu solder at 398 K. Adding Ni to the solder appears to make microstructural development finer and more uniform. The Ni added to the solder readily combined with Cu to form stable intermetallic compounds of $(Cu, Ni)_6Sn_5$ capable of improving the creep behavior of solder alloys. Moreover, microstructural characterization based on transmission electron microscopy analyses observing creep behavior in detail showed that such particles in the Sn-3.5Ag-0.5Cu-Ni-Ge solder alloy prevent dislocation and movement.

Key words: Sn-Ag-Cu-Ni-Ge lead-free solders, microstructure, creep, TH

INTRODUCTION

Many microelectronic products rely on solders to form critical electronic and mechanical connections between individual devices and on printed circuit boards. Virtually all solder joints are subject to temperature and power cycles during their service life. Moreover, electronic devices, particularly those used in vehicles and industrial products, are significantly more likely to encounter severe environments, including higher temperatures and fluctuating stresses and temperatures, which induce high-temperature creep and thermal fatigue in solder-joining materials.[1,2]

Creep deformation is the most common and critical deformation mechanism in solder joints, due to their higher homologous temperatures. Sn-Ag-Cu solders are subject to creep and recrystallization even at room temperature. In response, various techniques have been developed that involve the addition of trace amounts of Ni and Ge, which is believed to improve the high-temperature performance of solder alloys. Published reports have described the effects of adding Ge, which can prevent Sn oxidation and suppress dross formation in wave soldering.[3] Although the effects of adding Ni at the interface of solder joints have been studied,[4–7] little research has been done on the effects of adding Ni in bulk to Sn-Ag-Cu solder alloys.

This paper reports an investigation of the creep behavior of both bulk specimens and TH joints of Sn-3.5Ag-0.5Cu-Ni-Ge solder alloy, comparing this alloy with Sn-3.0Ag-0.5Cu solder alloy and addressing stress dependency and activation energy for creep in connection with microstructure observations to clarify the mechanism of deformation during creep. The paper also discusses investigations of particle growth behavior based on transmission electron microscopy (TEM Hitachi H9000UHR-I).

EXPERIMENTAL PROCEDURE

Table I gives the chemical composition of the materials used. We analyzed the composition of both solder alloys using a wavelength dispersive x-ray spectrometer (WDX Rigaku RIX 2000) and the technique of inductively coupled plasma spectrometry

(Received September 7, 2007; accepted January 20, 2009; published online February 7, 2009)

Table I. Chemical Compositions of Two Kinds of Solder Alloys (Mass %)

Alloy Code	Sn	Ag	Cu	Ni	Ge
Sn-3.5Ag-0.5Cu-Ni-Ge	Rem.	3.58	0.509	0.064	0.011
Sn-3.0Ag-0.5Cu	Rem.	3.07	0.522	–	–

Table II. Comparison of Typical Characteristics of Solders

	Sn-3.5Ag-0.5Cu-Ni-Ge	Sn-3.0Ag-0.5Cu
Solidus (K)	490	490
Liquidus (K)	494	492
Thermal expansion coefficient (1×10^{-6}/K)	22.3	21.7
Thermal conductivity (W/m K)	62	64

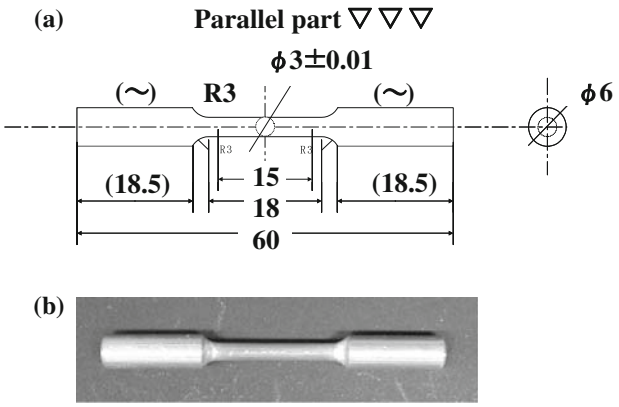

Fig. 1. Appearance of the bulk specimen: (a) shape of the specimen and (b) photo of the specimen.

(ICP PECTRO MODULA S). Table II summarizes the thermal characteristics of the Sn-Ag-Cu-Ni-Ge and Sn-Ag-Cu solder alloys.

Bulk Sample

The bulk creep specimens consisted of cast ingots of Sn-3.5Ag-0.5Cu-Ni-Ge and Sn-3.0Ag-0.5Cu solder alloys purchased from NIHON HANDA. Solder bars prepared by the manufacturer were melted in air in an electric furnace at 603 K for 2 h. The melt was then chill-cast as an ingot in a stainless-steel mold measuring 14 mm in diameter and 160 mm in length. The solder rods were machined into round creep specimens measuring 15 mm in length and 3 mm in diameter (Fig. 1). All specimens were heat-treated at 333 K for 24 h to remove residual stress and defects induced during specimen forming. Creep testing was performed at 313 K, 348 K, and 398 K, representing a homologous temperature

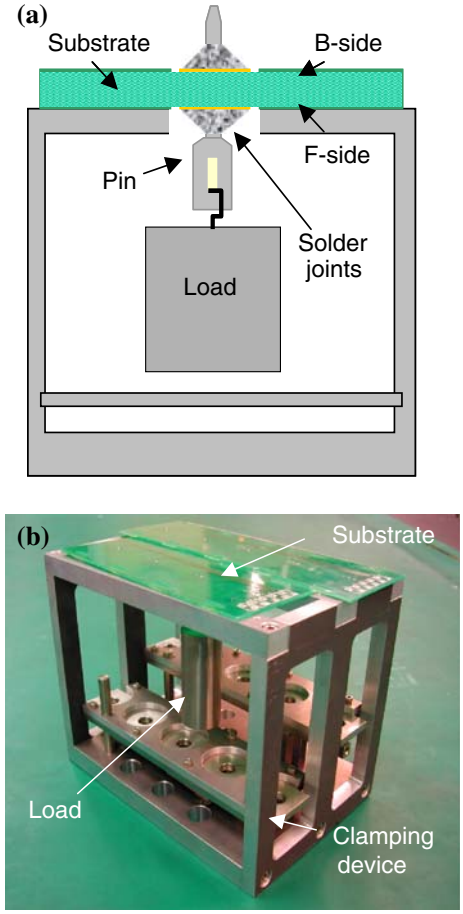

Fig. 2. Schematic diagram of TH joints creep test: (a) schematic of the device and (b) appearance of the test device.

η ($\eta = T/T_m$, where T_m is the melting point of the solder alloys) of 0.63, 0.71, and 0.81 for Sn-3.5Ag-0.5Cu-Ni-Ge and Sn-3.0Ag-0.5Cu, respectively. The stress range in the tests fell within 5–20 MPa, corresponding to a normalized stress of $\sigma/E = 10^{-5}$–10^{-3}, where E is Young's modulus.

TH Sample

Figure 2 shows the TH test specimen. Given the wide prevalence of through-hole (pin-in-hole) technology in the electronics industry, our study also incorporated creep tests of TH joints. The substrate material used for the TH test was a standard FR-4 epoxy–glass laminate of 195 mm × 120 mm × 1.6 mm. The Cu pads on the FR-4 substrate were 0.85 mm in diameter. The Cu pin measured 0.5 mm × 0.55 mm. Table III gives the wave-soldering conditions used. The wave-soldering temperature was set to 523 K, approximately 30 K above the melting point of the solder alloys.

Microstructural Examination

The samples were prepared for scanning electron microscopy (SEM) by wet grinding to #2400 grit sandpaper, followed by diamond particle polishing

Table III. Wave Soldering Condition

Surrounding	Atmosphere
Soldering temperature	523 K
Conveyor speed	16.7 mm/s
Conveyer angle	4°
Dip time	6 s
Flux	EC-19S-A

down to 0.25 μm, and a final polishing stage with a colloidal silica suspension. After polishing, samples were etched by Ar^+ ion milling and observed via SEM (Hitachi S 4300). We performed microstructural analyses of initial and creep-tested samples with TEM at an accelerating voltage of 300 kV. We also performed element mapping with an electron probe x-ray microanalyzer (Shimadzu EPMA 1610) to determine particle compositional characteristics.

RESULTS AND DISCUSSION

Creep Properties

Figure 3 shows creep curves up to the rupture times for the Sn-3.5Ag-0.5Cu-Ni-Ge and Sn-3.0Ag-0.5Cu solder alloys at temperatures of 313 K, 348 K, and 398 K at applied stresses of 5 MPa, 9.8 MPa, 14.7 MPa, and 19.8 MPa, respectively. TH creep tests were performed at temperatures of 313 K, 348 K, and 398 K under loads of 300 g, 400 g, 2000 g, and 3000 g, respectively. Only the creep rupture time was recorded for the TH solder joints. At the lower temperatures of 313 K and 348 K and higher stresses of 9.8 MPa to 19.8 MPa, creep rupture times for the Sn-3.0Ag-0.5Cu solder alloy were longer than for the Sn-3.5Ag-0.5Cu-Ni-Ge solder alloy. However, at the higher temperature of 398 K and lower stress of 5 MPa, the creep rupture time for the Sn-3.5Ag-0.5Cu-Ni-Ge solder alloy was approximately three times that of the Sn-3.0Ag-0.5Cu solder alloy.

Figure 4 shows the relationship between creep stress and creep-rupture time for the Sn-3.5Ag-0.5Cu-Ni-Ge and Sn-3.0Ag-0.5Cu solder alloys at each temperature. Table IV gives the creep results for the TH joints of both solder alloys at 398 K. These results show that adding Ni improved creep strength for the Sn-3.0Ag-0.5Cu solder alloy at higher temperatures.

Creep behavior can normally be characterized by a stress–strain rate relationship. The minimum creep rate $\dot{\varepsilon}_m$ is one of the most significant parameters of creep resistance in engineering assessments. Stress dependence is often described by the power-law equation:

$$\dot{\varepsilon}_m = A\sigma^n. \quad (1)$$

Here, $\dot{\varepsilon}_m$ is the minimum creep rate, while σ is applied stress, n is the stress exponent, and A is a material constant. Both A and n reflect temperature.

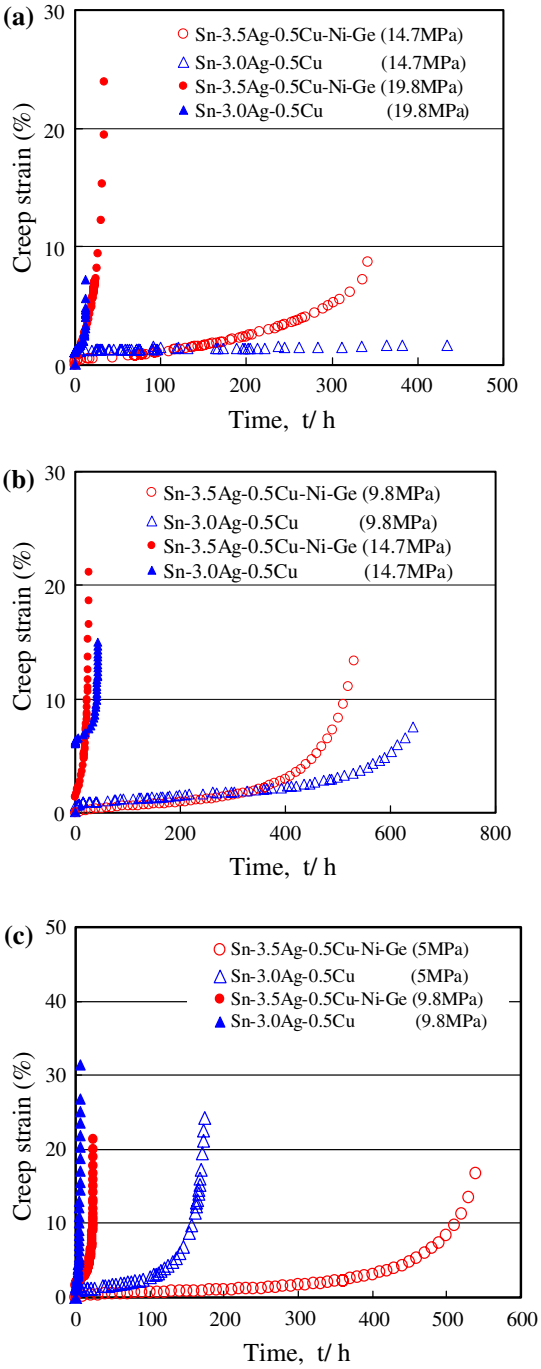

Fig. 3. Creep curves of the bulk of both solder alloys (a) creep-tested at 313 K, (b) creep-tested at 348 K, and (c) creep-tested at 398 K.

As expected, the creep rate increases progressively with stress at a given temperature and increases progressively with temperature at a given stress. Figure 5 clearly illustrates this relationship. Figure 5 shows the minimum creep rate as a function of applied stress of both solders at 313 K, 348 K, and 398 K, respectively. Figure 5a shows that the stress exponent of the Sn-3.5Ag-0.5Cu-Ni-Ge solder alloy declines with increasing temperature (from

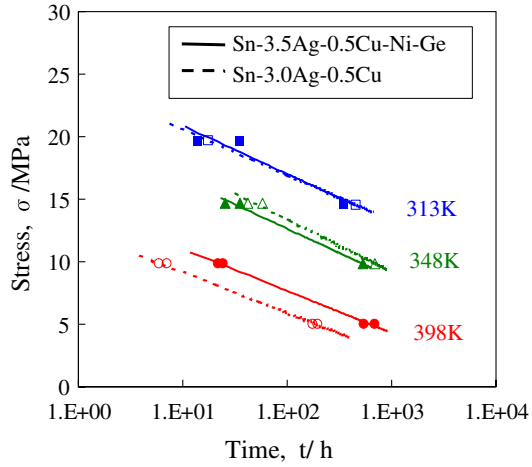

Fig. 4. Creep strength of the Sn-3.5Ag-0.5Cu-Ni-Ge solder alloy and the Sn-3.0Ag-0.5Cu solder alloy.

Table IV. Creep Results of the TH Joints of Both Solder Alloys at 398 K

Load (g)	Creep Rupture (h)			
	Sn-3.5Ag-0.5Cu-Ni-Ge		Sn-3.0Ag-0.5Cu	
300	500 (interrupted)		500 (interrupted)	
400	500 (interrupted)		500 (interrupted)	
2000	740	170 (interrupted)	168	153
3000	77	16	6	77

n = 11.3 at 313 K to n = 8.6 to 6.9 at 348 K to 398 K). On average, the stress exponent is approximately 8.9. Figure 5b also illustrates a tendency similar to that seen in Fig. 5a for the Sn-3.0Ag-0.5Cu solder alloy. The stress exponent of the Sn-3.0Ag-0.5Cu solder alloy is 5.1 at 398 K, 9.4 at 348 K, and 12.3 at 313 K. The creep mechanism of Sn-base solder alloys in the homologous temperature ranges from 0.63 to 0.81, and the stress range from $\sigma/G = 10^{-5}$ to 10^{-3} is in the dislocation-creep region.[8–12] The higher the n value of the stress exponent, the better the strengthening effect of the second phases in matrix Sn. Comparing the two solder alloys shows that the n value for the stress exponent for the Sn-3.5Ag-0.5Cu-Ni-Ge solder alloy is larger than that of the Sn-3.0Ag-0.5Cu solder alloy at 398 K, but less at 348 K and 313 K. We concluded that the microstructure of the Sn-Ag-Cu-Ni-Ge solder alloy is more stable than the Sn-Ag-Cu solder alloy at 398 K.

We can calculate the activation energy Q from the plot of $\ln(\dot{\varepsilon}_m)$ versus $1/T$, based on an Arrhenius-type equation (2). Figure 6 illustrates the results.

$$\dot{\varepsilon}_{\mathrm{m}} = A(\sigma/G)^n \exp(-Q/RT), \qquad (2)$$

where $\dot{\varepsilon}_{\mathrm{m}}$ is the minimum creep rate, A is a constant, σ is the applied stress, G is the temperature-dependent

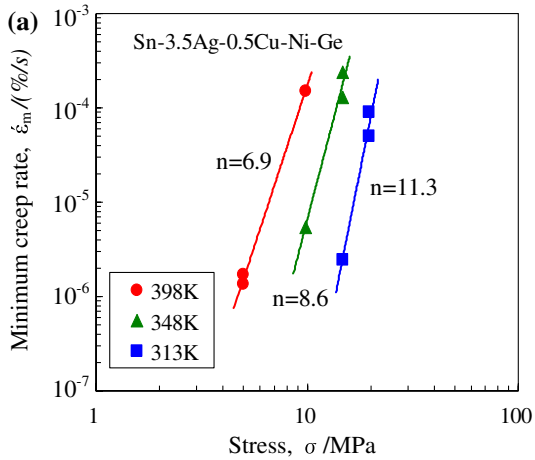

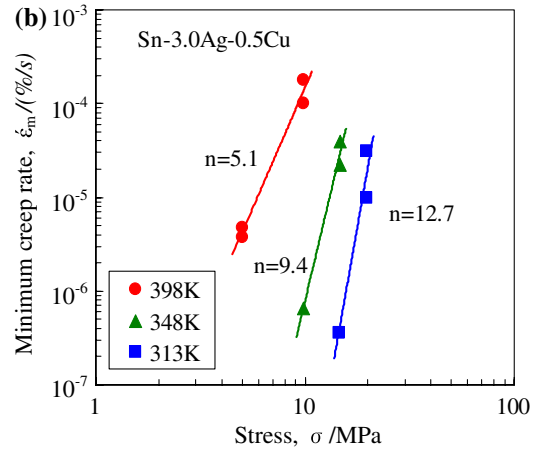

Fig. 5. Relationship between the stress and minimum creep rate of: (a) Sn-3.5Ag-0.5Cu-Ni-Ge and (b) Sn-3.0Ag-0.5Cu.

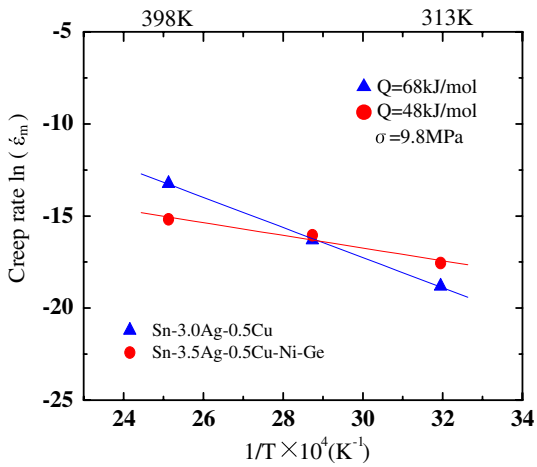

Fig. 6. Arrhenius plots of strain and reciprocal temperature of the Sn-3.5Ag-0.5Cu-Ni-Ge and the Sn-3.0Ag-0.5Cu solder alloys.

shear modulus, n is the stress exponent, Q is the apparent activation energy for creep, R is the universal gas constant, and T is absolute temperature. The apparent activation energy of creep for the Sn-3.5Ag-0.5Cu-Ni-Ge and Sn-3.0Ag-0.5Cu solder

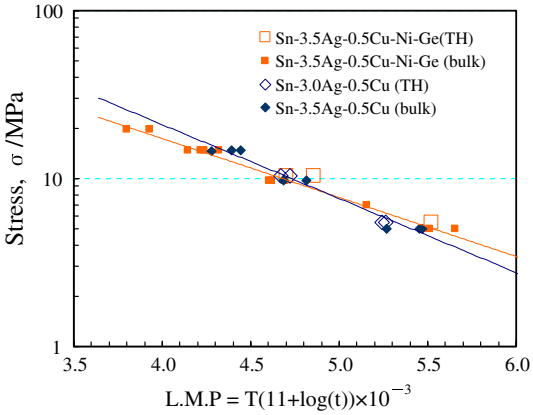

Fig. 7. Correlation of creep strength with Larson–Miller parameter.

alloys is 48 kJ/mol and 68 kJ/mol, respectively, under a constant stress of 9.8 MPa. In general, the lattice self-diffusion activation energy of pure tin is 102 kJ/mol, while the dislocation-pipe diffusion activation energy is about 0.6 times the lattice self-diffusion activation energy.[13–16] The apparent creep-activation energies for both solder alloys are lower and close to dislocation pipe diffusion. Moreover, the apparent activation energy for the Sn-3.0Ag-0.5Cu solder alloy is higher, implying that the microstructure of the Sn-3.0Ag-0.5Cu solder alloy is highly sensitive to creep temperature. The microstructure of the Sn-3.5Ag-0.5Cu-Ni-Ge solder alloy also appears more stable in the temperature range.[17,18]

The relationship among applied stress, temperature, and creep rupture time for bulk and TH joints in both solders can be plotted using Larson–Miller[19,20] plots. Figure 7 reflects all data. The Larson–Miller parameter (LMP) can be expressed as follows:

$$\mathrm{LMP} = T(C + \log(t)), \tag{3}$$

where T is absolute temperature, C is a constant (here 11), and t is creep rupture time.

Figure 7 shows that the creep strength of the Sn-3.5Ag-0.5Cu-Ni-Ge solder alloy is higher than that of the Sn-3.0Ag-0.5Cu solder alloy in regions of relatively higher temperatures and lower stress. The creep result of the bulk specimen corresponds to the TH joints.

Microstructure

We performed microstructural observations to clarify the relationship between creep strength and microstructure. Figure 8 shows an SEM micrograph of bulk specimens of both solders in their initial state. The microstructure of the Sn-3.5Ag-0.5Cu-Ni-Ge solder alloy shows two types of regions. The black-gray colored region is a dendritic β-Sn phase, while the light-colored region is a eutectic network band of dispersed Ag_3Sn and $(Cu, Ni)_6Sn_5$ intermetallic compounds (IMCs) within the β-Sn phase. This is finer and more uniform, and the hardness of the eutectic region is approximately 0.45 GPa, as

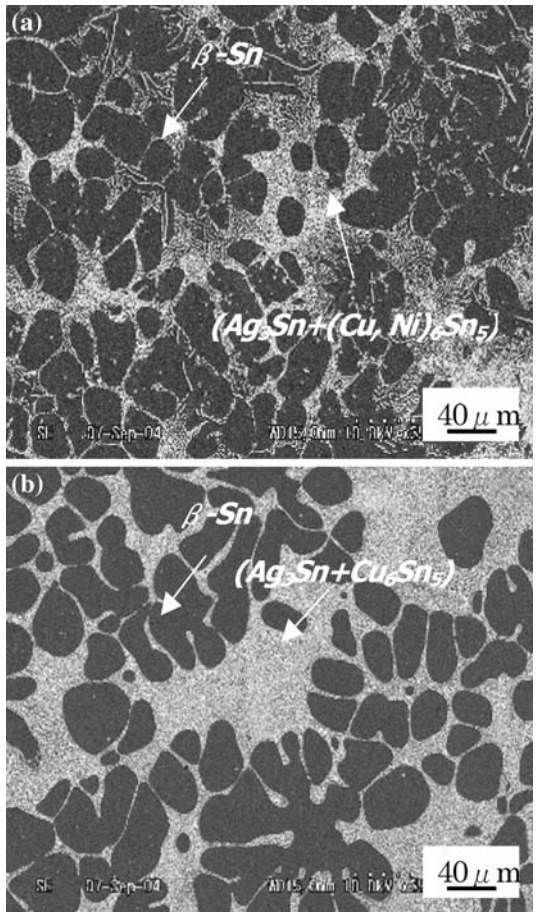

Fig. 8. Microstructure of the bulk specimen of the solder alloys: (a) Sn-3.5Ag-0.5Cu-Ni-Ge and (b) Sn-3.0Ag-0.5Cu.

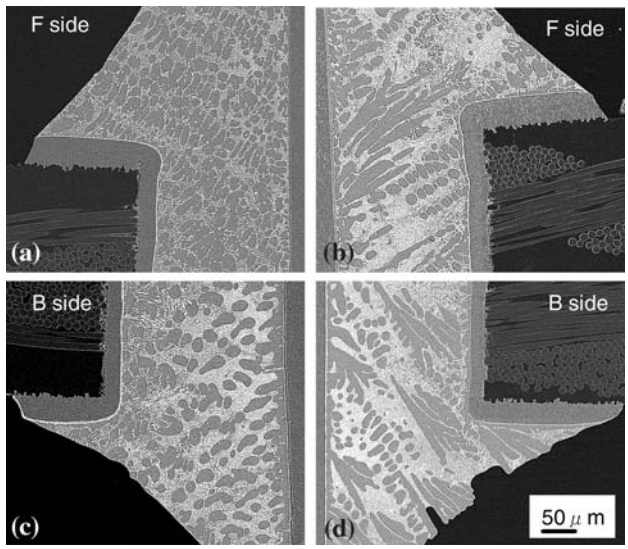

Fig. 9. Microstructure of cross section of the TH joints of both solder alloys: (a, c) Sn-3.5Ag-0.5Cu-Ni-Ge and (b, d) Sn-3.0Ag-0.5Cu.

determined by nanoindentation testing. On the other hand, we see segregated (larger block) eutectic regions of dispersed Ag_3Sn and Cu_6Sn_5 intermetallics within the β-Sn phase, which are dense

microstructures, in the Sn-3.0Ag-0.5Cu solder alloy from Fig. 8b, and the hardness of the segregated eutectic region is about 0.7 GPa. The deformation is unbalanced under applied stress.[21,22]

Figure 9 shows the microstructure of the TH joints for both solders after wave soldering. The microstructure of TH joints for Sn-3.0Ag-0.5Cu is also segregated, similar to the bulk sample. Shrinkage cracking is clearly visible from the

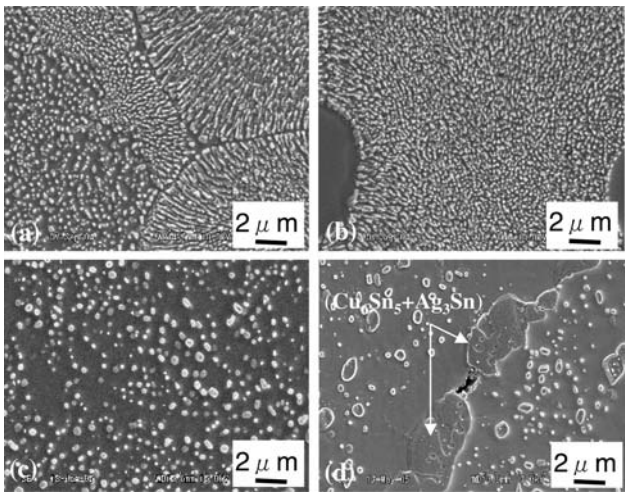

Fig. 10. SEM micrographs of the eutectic region of both solder alloys (a) Sn-3.5Ag-0.5Cu-Ni-Ge in initial state, (b) Sn-3.0Ag-0.5Cu in initial state, (c) Sn-3.5Ag-0.5Cu-Ni-Ge after creep testing at 398 K, 5 MPa for 200 h, and (d) Sn-3.0Ag-0.5Cu after creep testing at 398 K, 5 MPa for 180 h.

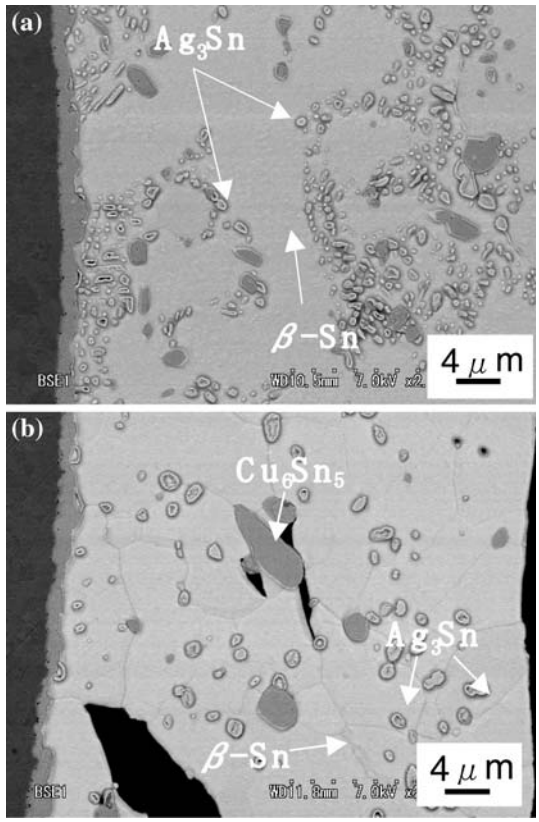

Fig. 11. BS graph of the TH joints of the two solder alloys: (a) Sn-3.5Ag-0.5Cu-Ni-Ge after creep testing at 398 K, 2000 g for 170 h and (b) Sn-3.0Ag-0.5Cu after creep testing at 398 K, 2000 g for 170 h.

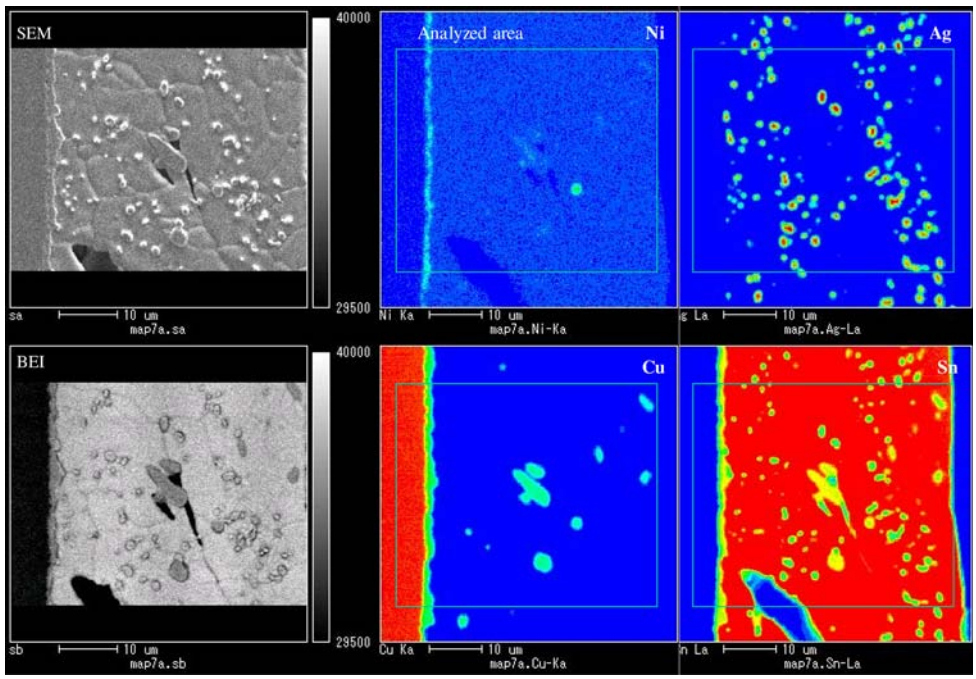

Fig. 12. EPMA mapping analysis of the TH joints of the Sn-3.0Ag-0.5Cu solder alloy after creep testing at 398 K, 2000 g for 170 h.

surface and cross sections of TH joints, whereas the TH joint of the Sn-3.5Ag-0.5Cu-Ni-Ge solder alloy shows a finer and more uniform microstructure than the Sn-3.0Ag-0.5Cu solder alloy.

Figure 10 shows an SEM image of a eutectic region of the Sn-3.5Ag-0.5Cu-Ni-Ge solder alloy and the Sn-3.0Ag-0.5Cu solder alloy in the initial state and after the creep test at 398 K, 5 MPa. Before the creep test, although the microstructure of the Sn-3.0Ag-0.5Cu solder alloy has a higher concentration of Ag_3Sn particles than the Sn-3.5Ag-0.5Cu-Ni-Ge solder alloy, both solder alloys have fine microstructures in the eutectic regions. The particle size for both solder alloys became coarser after a creep test at 398 K, 5 MPa. Of special note here is the appearance and significant growth of Cu_6Sn_5 IMCs in the Sn-3.0Ag-0.5Cu solder alloy.[23] The apparent difference in creep rupture strength between the Sn-3.5Ag-0.5Cu-Ni-Ge solder alloy and the Sn-3.0Ag-0.5Cu solder alloy at high temperature (398 K) and low stress (5 MPa) depends on the size and the stability of the particles in the eutectic region. For cases of higher temperature and lower stress, Cu_6Sn_5 IMCs grow rapidly in the eutectic region of the Sn-3.0Ag-0.5Cu solder alloy, while the cavities or cracks generated by the coarser particles propagate, and creep rupture occurs within a shorter time. On the other hand, no particles resembling coarse Cu_6Sn_5 were observed in the Sn-3.5Ag-0.5Cu-Ni-Ge solder alloy. This appears to be attributable to the addition of Ni to the Sn-3.0Ag-0.5Cu solder alloy.

Figure 11 shows a similar comparison for TH joints of both solders after creep testing at 398 K, 2000 g for 170 h. We saw significant microstructural changes as well in the TH joints of the Sn-3.0Ag-0.5Cu solder alloy. The particles of Cu_6Sn_5 IMCs[23] in the Sn-3.0Ag-0.5Cu solder grew faster than those of the $(Cu, Ni)_6Sn_5$ IMCs in the Sn-3.5Ag-0.5Cu-Ni-Ge solder. To analyze the elemental make-up of the particles, we performed EPMA mapping analysis in the same areas of the TH joints of the Sn-3.0Ag-0.5Cu solder alloy. Figure 12 shows the result of EPMA analysis. Cu and Sn were detected from markedly coarsened particles, but the presence of Ni could not be confirmed. The coarsened particles are Cu_6Sn_5 IMCs.[24]

We performed TEM analysis to investigate the relationship between creep strength properties and precipitates. Figure 13 shows a TEM image of a Sn-3.5Ag-0.5Cu-Ni-Ge solder alloy in its initial state and after creep testing at 398 K. At the initial state, particle sizes are 0.1 μm to 0.2 μm. These particles grow to 0.5 μm to 1.0 μm after the creep test at 398 K and 5 MPa for 550 h, with dimensions severalfold larger than in the initial state. We also observed particles blocking dislocations and confirmed that particles measuring approximately 0.5 μm in diameter are $(Cu, Ni)_6Sn_5$ IMCs in the Sn-3.5Ag-0.5Cu-Ni-Ge solder alloy.[25] The smaller particles appear to improve creep strength.

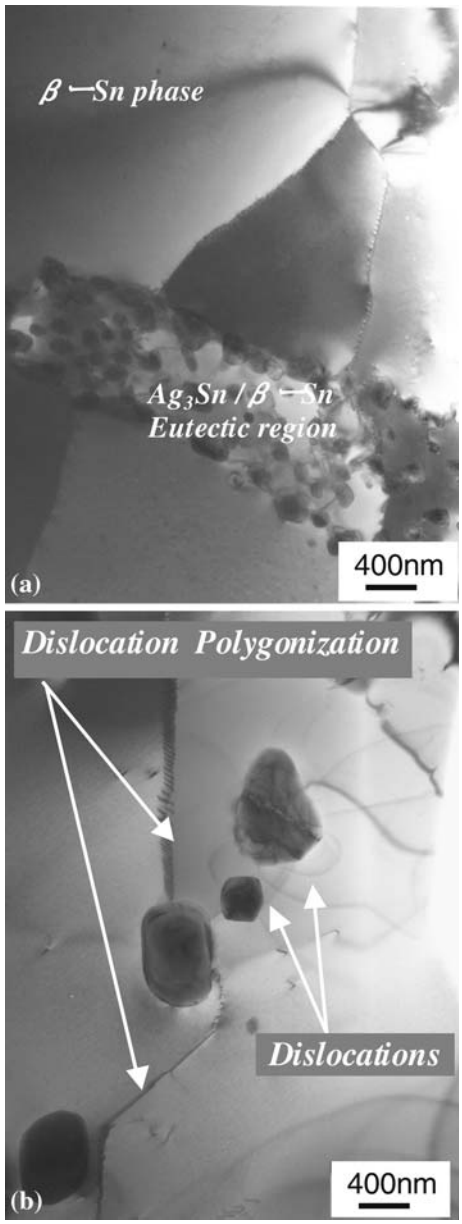

Fig. 13. TEM graph of the Sn-3.5Ag-0.5Cu-Ni-Ge solder alloy: (a) initial state, (b) after creep testing at 398 K, 5 MPa for 550 h.

CONCLUSION

Our study compared the relationship between the microstructural and creep behavior of bulk specimens and TH joints for Sn-3.5Ag-0.5Cu-Ni-Ge and Sn-3.0Ag-0.5Cu solder alloys. We arrived at the following conclusions.

We examined the creep behavior of both solders in the 313 K to 398 K temperature range and $\sigma/E = 10^{-5}$ to 10^{-3} stress range. The creep strength of Sn-3.5Ag-0.5Cu-Ni-Ge solder alloy at 398 K is approximately three times that of the Sn-3.0Ag-0.5Cu solder alloy. Moreover, we can link the creep strength of the bulk specimen and creep strength of the TH joints sample using an LMP plot.

The stress exponents of the Sn-3.5Ag-0.5Cu-Ni-Ge solder alloy and the Sn-3.5Ag-0.5Cu solder alloy were 6.9 and 5.1, and their apparent activation energies at 9.8 MPa were 48 kJ/mol and 68 kJ/mol, respectively. The microstructure of the Sn-3.0Ag-0.5Cu solder alloy appears quite sensitive to creep temperature.

The initial microstructure of the Sn-3.5Ag-0.5Cu-Ni-Ge solder alloy is finer and more uniform than that of the Sn-3.0Ag-0.5 solder alloy.

Creep characteristics were apparently affected by IMC growth in the eutectic region. The IMCs of $(Cu, Ni)_6Sn_5$ formed after the addition of Ni showed improved creep strength at regions of higher temperature (398 K) and lower stress (5 MPa).

ACKNOWLEDGEMENTS

The authors wish to thank Dr. Kariya (Shibaura Institute of Technology) for helpful insights shared during various discussions.

REFERENCES

1. National Center for Manufacturing Sciences, "Lead-Free Solder Project Final Report," NCMS Report 0401RE96, August (1997).
2. Lead-Free Soldering Roadmap Committee of JEITA, "Lead-Free Roadmap 2002," official version2.1, September (2002).
3. M. Nagano, N. Hidaka, M. Shimoda, and H. Watanabe, *Proceedings of New Frontiers of Process Science and Engineering in Advanced Materials* (Japan: High Temperature Society of Japan, 2004), pp. 256–261.
4. T.T. Mattila and J.K. Kivilahti, *J. Electron. Mater.* 34, 969 (2005).
5. T.H. Chuang, S.F. Yen, and M.D. Cheng, *J. Electron. Mater.* 35, 302 (2006).
6. S. Terashima and M. Tanaka, *Mater. Trans.* 45, 681 (2004).
7. I. Shoji, S. Tsunoda, H. Watanabe, T. Asai, and M. Nagano, *Mater. Trans.* 46, 2737 (2005).
8. V.I. Igoshev and J.I. Kleiman, *J. Electron. Mater.* 29, 244 (2000).
9. C.M.L. Wu and M.L. Huang, *J. Electron. Mater.* 31, 442 (2002).
10. M. Kerr and N. Chawla, *Acta Metall.* 52, 4527 (2004).
11. R.J. Mccabe and M.E. Fine, *Metall. Mater. Trans.* 33A, 1531 (2002).
12. K. Atsumi, Y. Kariya, and M. Otsuka, *Proceedings of 6th Symposium on Microjoining and Assembly Technology in Electronics* (Japan: The Japan Welding Society, 2000), pp. 281–286.
13. Y. Kariya, M. Otsuka, and W.J. Plumbride, *J. Electron. Mater.* 32, 1398 (2003).
14. I. Shohji, T. Yoshida, T. Takahashi, and S. Hioki, *Proceedings of 9th Symposium on Microjoining and Assembly Technology in Electronics* (Japan: The Japan Welding Society, 2003), pp. 229–234.
15. Z. Chen, Y. Shi, and Z. Xia, *J. Electron. Mater.* 33, 964 (2004).
16. F. Ochoa, X. Deng, and N. Chawla, *J. Electron. Mater.* 33, 1596 (2004).
17. P.T. Vianco, J. Rejent, and A.C. Kilgo, *J. Electron. Mater.* 33, 1389 (2004).
18. Q. Xiao and W.D. Armstrong, *J. Electron. Mater.* 34, 196 (2005).
19. D. Mitlin, C.H. Raeder, and R.W. Messler Jr., *Metall. Mater. Trans.* 30A, 115 (1999).
20. R. Ninomaya, Y. Nakahara, and T. Takemoto, *Proceedings of 9th Symposium on Microjoining and Assembly Technology in Electronics* (Japan: The Japan Welding Society, 1998), pp. 249–252.
21. M. Nagano, N. Hidaka, M. Shimoda, and M. Ono, *J. Jpn Inst. Electr. Packag.* 8, 495 (2005).
22. M. Nagano, N. Hidaka, H. Watanabe, M. Shimoda, and M. Ono, *J. Jpn Inst. Electr. Packag.* 9, 171 (2006).
23. M. Shimoda, K. Matusmura, and T. Nakanisi, *Proceedings of 9th Symposium on Microjoining and Assembly Technology in Electronics* (Japan: The Japan Welding Society, 2003), pp. 325–330.
24. N. Hidaka, H. Watanabe, M. Shimoda, M. Ono, and M. Nagano, *Proceedings of 12th Symposium on Microjoining and Assembly Technology in Electronics* (Japan: The Japan Welding Society, 2006), pp. 235–238.
25. N. Hidaka, M. Nagano, M. Shimoda, H. Watanabe, and M. Ono, *Proceedings of ASME/Pacific Rim Technical Conference and Exhibition on Integration and Packaging of MEMS, NEMS, and Electronic Systems* (San Francisco, CA: ASME, InterPACK, 2005), p. 73148.